Investigation of a Hybrid OFDM-PWM/PPM Visible Light Communications System

Farzane Ebrahimi[1], Zabih Ghassemlooy[2], *Senior Member, IEEE*, and Saeed Olyaee[1,*], *Member, IEEE*

[1]Nano-photonics & Optoelectronics Research Lab. (NORLab), Shahid Rajaee Teacher Training University, Lavizan, Tehran, Iran.
[2]Optical Communications Research Group, Faculty of Engineering and Environment, Northumbria University, Newcastle upon Tyne NE1 8ST, U.K.

Abstract
In visible light communications with the optical orthogonal-frequency-division multiplexing (O-OFDM) technique, the high peak-to-average-power-ratio (PAPR) is an important issue due to the limited dynamic range of light emitting diode (LED)-based light sources. To address this problem, we propose a hybrid OFDM-pulse time modulation (PTM) scheme where bipolar O-OFDM samples are converted into the digital PTM formats of pulse width modulation (PWM) and pulse position modulation (PPM) for the intensity modulation of LEDs. We convert the DC biased optical OFDM (DCO-OFDM) and asymmetrically clipped optical OFDM (ACO-OFDM) samples to PTM and show that DCO-OFDM-PTM offers improved bit error rate (BER) performance. For example, for 16-quadrature amplitude modulation (QAM) at the BER of 10^{-3}, the signal-to-noise ratio (SNR) gains are ~1.35 dB and ~1 dB for DCO-OFDM-PPM and DCO-OFDM-PWM compared to ACO-OFDM-PPM and ACO-OFDM-PWM, respectively. Simulation results show that DCO-OFDM-PPM displays an improved BER performance compared with DCO-OFDM-PWM for both lines of sight (LOS) and diffuse configurations. For instance, for an ideal LOS channel and for 16- QAM at the BER of 10^{-3}, the required SNR values are ~4.5 and ~10.2 dB for DCO-OFDM-PPM and DCO-OFDM-PWM, respectively.

Keyword: Visible Light Communications; Optical Wireless Communications; hybrid OFDM-PPM; hybrid OFDM-PWM; PAPR

1. Introduction

Radio frequency (RF)-based wireless technologies have a limited and costly spectrum. Since data traffic is growing exponentially at a global level, new and complementary wireless communication techniques are being considered [1]. Due to the rapid progress of solid-state lighting technology, optical wireless communications (OWC) have become a potentially viable solution for certain applications in recent years [2]. In indoor environments, the visible light communications (VLC) technology based on light emitting diode (LED) lighting fixtures provides data communications, indoor localization, and illumination, thus resulting in both energy and cost saving while reducing the burden on the utilization of the RF spectrum [3].

There are three major challenges in VLC: (*i*) the low modulation bandwidth of LEDs (B_{LED}<5 MHZ) which leads to a limited transmission capacity [4]; (*ii*) the nonlinear power-current (*P-I*) characteristics of LEDs which results in current amplitude-dependent DC offset, amplitude offset at each subcarrier, frequencies' harmonic distortion, and intermodulation products [5]; and (*iii*) multipath-induced intersymbol interference (ISI) [6]. A number of options exists for overcoming the 1st and 2nd challenges, including (*i*) high spectrally efficient multi-carrier modulation schemes such as optical OFDM, discrete multitone, and multi-band carrierless amplitude and phase

modulation [7]-[10]; (*ii*) parallel transmission multiinput-multioutput (MIMO) [11]-[12] and color-clustered MIMO techniques [13]; (*iii*) pre-, post- and adaptive equalization [14]-[15]; (*iv*) blue filtering [16]; and (*v*) red, green, and blue LEDs [17] as well as micro-LEDs [18]. The mitigation schemes for the 3rd challenge are pre-distortion, Volterra equalization, and adoptive post-distortion schemes [19]-[21].

In VLC, LEDs can only be intensity-modulated (IM) with real and positive input signals. Conventional OFDM signals are bipolar and complex and cannot be used for the IM of LEDs. OFDM signal formats are highly sensitive to the LED's nonlinearity due to their high peak-to-average power ratio (PAPR). This leads to severe non-linear signal distortion and a large DC-bias that can seriously degrade the power efficiency of VLC systems and affect system performance due to the very limited dynamic range of LEDs [22]. It also reduces throughput due to the use of longer cyclic prefix because of longer tails of the channel impulse response [23]. Note that, there are several modified formats of OFDM with non-negative real values such as DC-biased optical OFDM (DCO-OFDM) and asymmetrically clipped optical OFDM (ACO-OFDM) [5]. A number of techniques have been proposed to address the need for a higher PAPR, including pilot symbol, selected mapping, discrete sliding norm transform, and subcarrier grouping [24]-[29].

Compared to RF outdoor channels, an indoor VLC environment is relatively static with very little movement of people and the availability of both line of sight (LOS) and non-line of sight (NLOS) paths, thus resulting in almost no deep and fast fading and very little multipath-induced interference [30]. Therefore, the justification for adopting OFDM in indoor VLC would be to increase the data rate but at the cost of a higher PAPR and increased system complexity. However, PAPR can be resolved by adopting a hybrid OFDM-PTM scheme where OFDM is converted to a digital format, which is ideal for switching LEDs regardless of their *P-I* characteristics. In [31], the OFDM-PWM scheme was experimentally investigated where a linear mapping function was used to convert ACO-OFDM into pulse width modulation (PWM) and the results were compared with the original ACO-OFDM. Since the PWM signal can be bipolar, the ACO-OFDM time domain property was used and only the first half of the samples were converted to PWM with no zero clipping. In order to ensure that the required transmission bandwidth of OFDM-PWM is the same as that of ACO-OFDM, the PWM pulse width was extended by the number of subcarriers N_{sc}. We showed that OFDM-PWM is more resilient to LED nonlinearity with reduced PAPR and improved bit error rate (BER) performance compared with the original ACO-OFDM. For example, at the BER of 10^{-4} for OFDM-PWM with 16- and 64-quadrature amplitude modulation (QAM), the signal-to-noise ratio (SNR) gains were ~ 4 dB and ~9 dB, respectively, compared with ACO-OFDM.

In the present study, we extended the investigation to include DCO-OFDM and ACO-OFDM by converting them to PWM and pulse position modulation (PPM) formats. We showed that, at the BER of 10^{-3} for DCO-OFDM-PPM, the SNR gains are ~ 0.3, ~ 0.7, ~ 1.65, and ~ 3.5 dB, compared with DCO-OFDM-PWM for *M* of 8, 16, 64, and 256, respectively. However, for DCO-OFDM-PWM at the BER of 10^{-3}, the SNR gains are ~ 1 dB compared with ACO-OFDM-PWM for *M*=16. The rest of the paper is organized as follows: OFDM-PPM is introduced and compared with OFDM-PWM in Section 2. In Section 3, we outline the simulation of both schemes for LOS and NLOS (diffuse) configurations and show that OFDM-PPM is more resistant against ISI and offers an improved BER performance. The concluding remarks are given in the final section.

2. OFDM with PWM and PPM

As shown in Figure 1, there are a number of pulse modulation schemes that can be adopted in hybrid schemes. OOK is the simplest technique, where the intensity of an optical source is directly modulated by the information sequence. In contrast, PTM techniques use the information sequence to vary some time-dependent property of a pulse train. In PWM and PPM the sample values determine the pulse width and the position of a narrow pulse, respectively. In digital pulse interval modulation (DPIM), the information is represented by the number of empty slots between pulses. DPIM potentially offers higher data rates and improvements in power efficiency compared to OOK and PPM. The differential PPM (DPPM), which can be considered as inverted DPIM improves the power efficiency as well as the bandwidth efficiency or the throughput by removing all the empty slots that follow a pulse in a PPM symbol. The pulse frequency modulation

(PFM) controls the frequency of the narrow pulses as shown in Figure 1. Square wave frequency modulation (SWFM) is closely related to both PFM and analogue FM, consisting essentially of a series of square wave edge transitions occurring at the zero crossing points of FM [32].

Here, we only considered the most widely used schemes of PWM and PPM. In PWM, the information $d(t)$ is transmitted by varying the width τ of a constant amplitude pulse stream $s(t)$. The average pulse duration $\overline{\tau} = (L-1)T_s/2$ where $T_s = T_f/L$ is the slot duration, $T_f = MR_b^{-1}$ is the symbol length, $L = 2^M$, and M is the bit resolution. In PPM, which is the differentiated version of PWM, the position of a short pulse of duration T_s within the fixed symbol period conveys the information. PPM is more power-efficient (i.e., has a lower average power and therefore a lower PAPR) than PWM and is most suitable for LOS links, although at the cost of increased channel bandwidth requirement and system complexity (i.e. the need for system synchronization). The bandwidth requirement (normalised to NRZ-OOK) of PWM and PPM are 2/3 and $2^M/M$, respectively [33]. Note that, in VLC systems under full brightness, the PPM data format is not suitable because of the difficulty in controlling the brightness level of LEDs. To overcome this, a variable PPM scheme, which is a combination of PWM and PPM, can be used to provide brightness control [34].

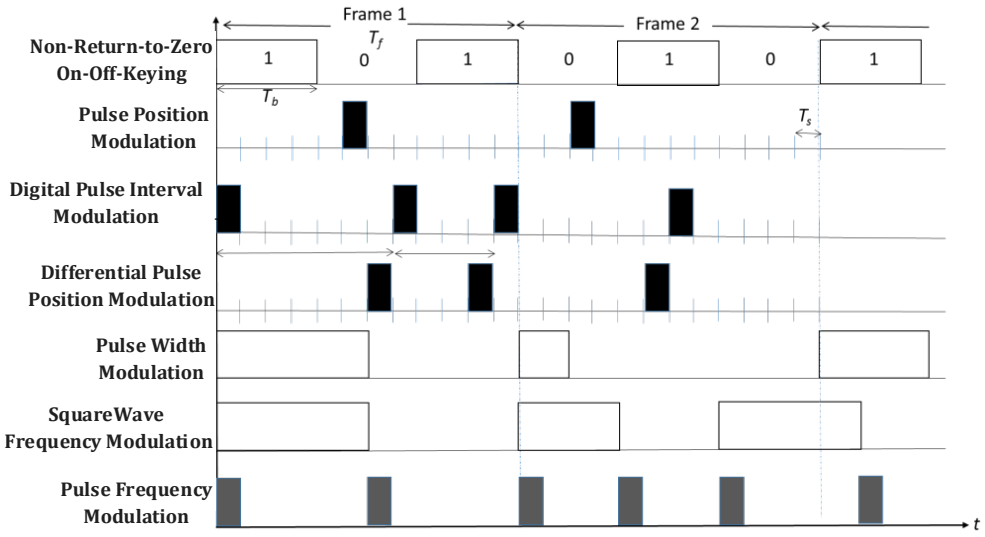

Figure 1: Pulse time modulation formats

The PWM and PPM pulse shapes are given by:

$$s_{pwm}(t) = \begin{cases} A, & 0 \le t \le \alpha T_s \\ 0, & \alpha T_s \le t \le LT_s \end{cases} \qquad \alpha = 1,2,3 \ldots L \tag{1}$$

$$s_{ppm}(t) = \begin{cases} 0, & t \le nT_s \\ A, & nT_s \le t \le (n+1)T_s \end{cases} \tag{2}$$

where $n \in \{1, 2, 3 \ldots L\}$ and A is the pulse peak amplitude.
The PWM and PPM symbols are given as:

$$x(t)_{PWM} = L\overline{P}\sum_{k=0}^{L-1} C_k s_{pwm}(t - \alpha T_s) \tag{3}$$

$$x(t)_{PPM} = L\overline{P}\sum_{k=0}^{L-1} C_k s_{ppm}(t - kT_s) \tag{4}$$

where $C_k \in \{0,1,2.....2^M - 1\}$ shows the data sequence, $\overline{P}$ denotes the average power, and $L\overline{P}$ represents the peak power.

The block diagram of the proposed OFDM-PTM scheme is illustrated in Figure 2. We adopted the standard OFDM building blocks. Therefore, we do not describe them here (More on this can be found in [35]). In ACO-OFDM, the output of IFFT is a real-valued signal with only the odd

harmonics being loaded. The digital signal at the input to DAC is the sequence of OFDM symbols with N time domain samples given by [7]:

$$x_k = \frac{1}{N}\sum_{n=1}^{\frac{N}{2}-1} X_n exp\{-2\pi ikn/N\} + c.c. \ \ , k = 0,1, \dots N-1 \tag{5}$$

where N is the size of FFT.

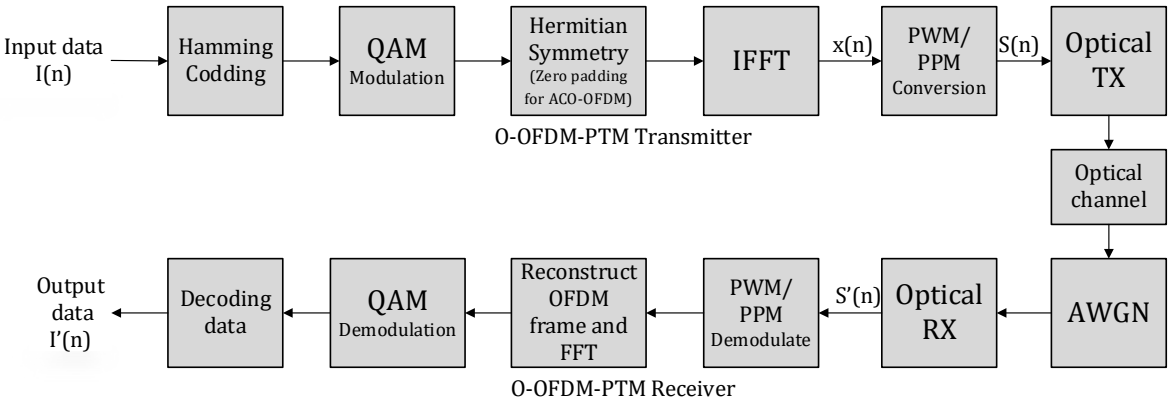

Figure 2: Block diagram of hybrid OFDM-PTM scheme

The OFDM symbol is the superposition of Fourier harmonics (subcarriers) with complex amplitudes X_n that are constrained to have Hermitian symmetry $X_n = X^*_{N-n}$ in order to produce real-valued signal samples x_k. The bipolar signal at the output of DAC is characterized by a high PAPR, particularly when the number of non-zero subcarriers is large. Applying such a signal directly to the IM light source would lead to large distortions of the optical signal. In order to avoid these distortions, a positive DC component I_{DC} has to be added to the analog signal, i.e., $y_n = x_n + I_{DC}$. Note that adding I_{DC} will only affect the DC component X_0 that has no data. This is a drawback since it leads to a substantial drop in power efficiency. Therefore, this requires that the response characteristics of both the transmitter and the receiver should have a linear dynamic range $[I_{\min}, I_{\max}] \geq$ PAPR, where $I_{\min}$ and $I_{\max}$ denote minimum and maximum LED drive currents, respectively. A high PAPR, which is a random variable and changes symbol by symbol, represents the serious drawback of the OFDM technique, which is defined as [36]:

$$PAPR \triangleq \frac{\max\limits_{0\leq n\leq N-1} |x[n]|^2}{\sigma_x^2} \tag{6}$$

where σ_x^2 is the variance of x_n.

DCO-OFDM samples are mapped into PWM/PPM symbols where the sample values determined the pulse width and the location of PWM and PPM, respectively. Note that, there is no DC-biasing or zero clipping. In ACO-OFDM, because of its anti-symmetry property, only the first half of bipolar samples are mapped into PWM/PPM with no zero clipping. The generated hybrid OFDM-PWM/PPM signal is used for the IM of LEDs. The ACO-OFDM signal with the anti-symmetry property is given by [7]:

$$x_k = x_{k+N/2} \qquad 0 < k < N/2 \tag{7}$$

where N is the number of IFFT points. The generated OFDM-PWM/PPM signal is utilized for the IM of LEDs.

To simplify the conversion of O-OFDM samples into PWM/PPM symbols, the symbol duration is divided into L number of slots. OFDM-driven PWM and PPM signals are given by [37]:

$$s_{PWM}(n) = \begin{cases} C & 0 \leq N_{s(n)} \leq N_\tau \\ 0 & N_\tau < N_{s(n)} \leq L \end{cases} \tag{8}$$

$$s_{PPM}(n) = \begin{cases} 0 & 0 \leq N_{s(n)} \leq N_\tau \\ C & N_\tau < N_{s(n)} \leq N_\tau + 1 \\ 0 & N_\tau + 1 < N_{s(n)} \leq L \end{cases} \tag{9}$$

where $N_{S(n)}$ is the number of time slots in PWM and PPM symbols. N_τ, which determines the pulse width in PWM or pulse position in PPM is given by:

$$N_\tau = \frac{x(n) - x_{max}}{x_{max} - x_{min}} \times L \tag{10}$$

where x_{min} and x_{max} are the maximum and minimum amplitudes of O-OFDM symbols, respectively. The time domain waveform of the DCO-OFDM-PWM scheme is illustrated in Figure 3.

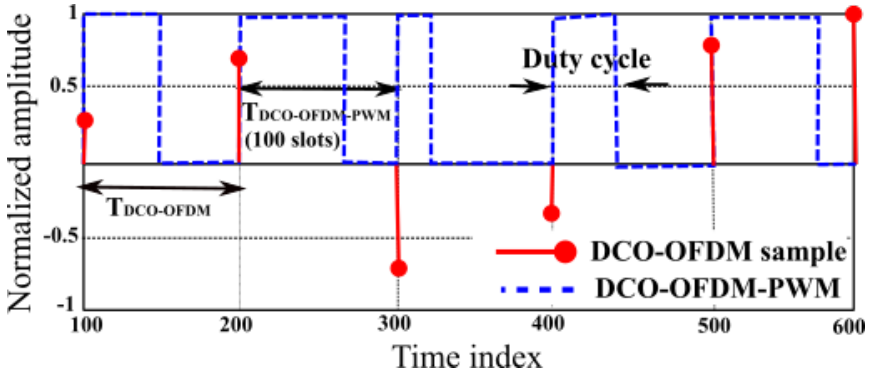

Figure 3: Time domain waveform for DCO-OFDM and DCO-OFDM-PWM

In both PWM and PPM schemes, the minimum pulse duration is $1/L$ times smaller than O-OFDM. Therefore, the required bandwidth of OFDM-PWM/PPM is L times larger than that of O-OFDM. In order to reduce the required bandwidth, the duty cycle is extended by a factor of N_C, in which $0 \leq N_c \leq L$. In this case, OFDM-PWM and PPM signals are given by:

$$s_{PWM}(n) = \begin{cases} c & 0 \leq N_{s(n)} \leq N_\tau + N_c \\ 0 & N_\tau + N_c < N_{s(n)} \leq L + N_c \end{cases} \tag{11}$$

$$s_{PPM}(n) = \begin{cases} 0 & 0 \leq N_{s(n)} \leq N_\tau \\ c & N_\tau < N_{s(n)} \leq N_\tau + N_c + 1 \\ 0 & N_\tau + N_c + 1 < N_{s(n)} \leq L + N_c \end{cases} \tag{12}$$

For $N_C = L$, the required bandwidth of OFDM-PWM/PPM is the same as that of O-OFDM. Following optical detection, the received OFDM-PWM/PPM signal is given by:

$$s(n) = s(n) \otimes h(n) + z(n) \tag{13}$$

where $h(n)$ is the channel impulse response, $z(n)$ is the additive white Gaussian noise (AWGN) with zero mean, and $\otimes$ denotes the convolution operation. At the receiver, following OFDM extraction, we adopted the standard OFDM demodulation process as in [33].

PAPR is a key factor influencing the performance of OOFDM systems and is defined as the ratio of the maximum instantaneous power to average power, characterized by the complementary cumulative distribution function (CCDF) as given by [6]:

$$CCDF = P(PAPR > PAPR_0) = 1 - P(PAPR \leq PAPR_0) = 1 - CDF \tag{14}$$

where $PAPR_0$ is the threshold (reference) PAPR.

3. Simulation results

In this paper, we considered a room with the dimensions of 5×5×3 (length, width, and height, in that order) with two configurations (Figure 4). We employed Matlab to evaluate the performance of the proposed schemes. All key simulation parameters are presented in Table 1, and the flowchart of OFDM-to-PTM conversion is illustrated in Figure 5.

The duration of slots is given by:

$$T_{slot} = \frac{time\ duration\ of\ OFDM\ signal / number\ of\ sample\ in\ OFDM\ signal}{number\ of\ slot\ in\ PWM\ or\ PPM\ symbol} \tag{15}$$

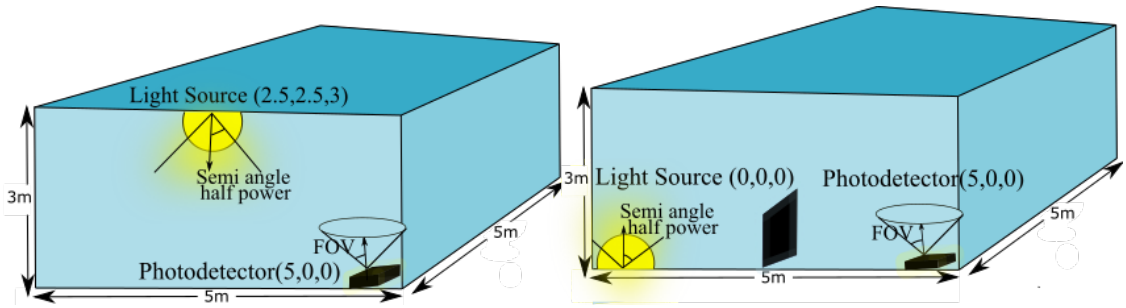

Figure 4: Proposed system configurations: (a) line of sight, and (b) non-line of sight

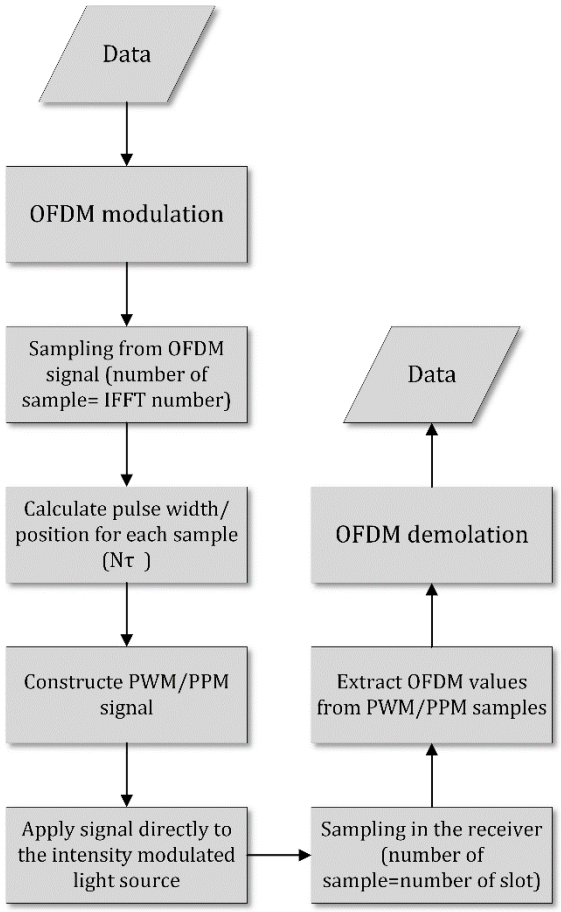

Figure 5: The flowchart of OFDM to PTM conversion

Table 1: Simulation parameters

Parameter	Value
Modulation	4, 8, 16, 64, 256 QAM
FFT/IFFT size	256
Number of subcarrier (N_{SC})	256
Number of slots per PTM symbols (L)	100
Extended factor	10
Symbol rate	36×10^{6} symbol/second
Slot duration	2.5×10^{-10} s
Signal duration of PWM/PPM	$110 \times 2.5\times10^{-10}$ s
Pulse width of PPM	2.5×10^{-9} s
Pulse width of PWM	2.5×10^{-9} _ 2.7×10^{-8} s
Iteration	1000

Figure 6 shows CCDF against PAPR for 64-QAM DCO-OFDM-PWM, DCO-OFDM-PPM, and ACO-OFDM schemes. Note that, the number of IFFT points was set to 256. The PAPR values for PWM and PPM are ~3 dB and ~10 dB, respectively.

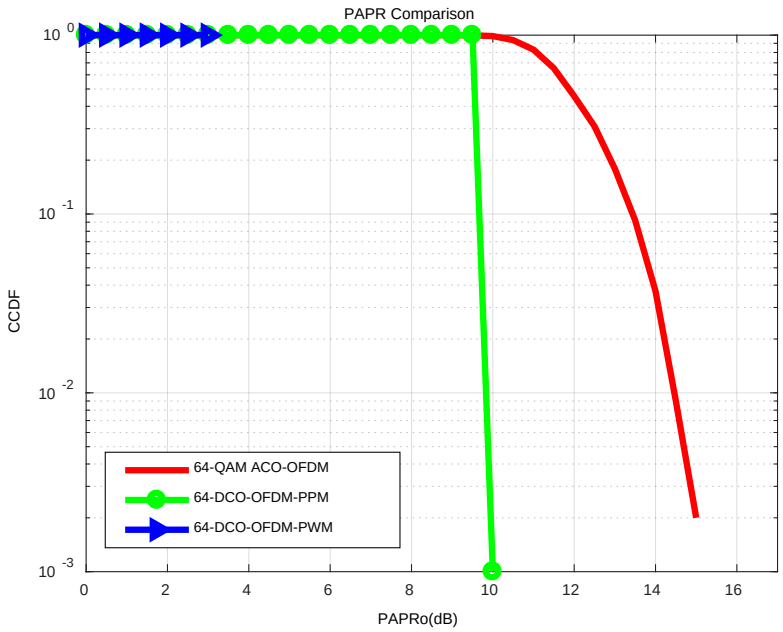

Figure 6: PAPR analysis for original ACO-OFDM, DCO-OFDM-PWM and DCO-OFDM-PPM (N_{SC}=256, L=100).

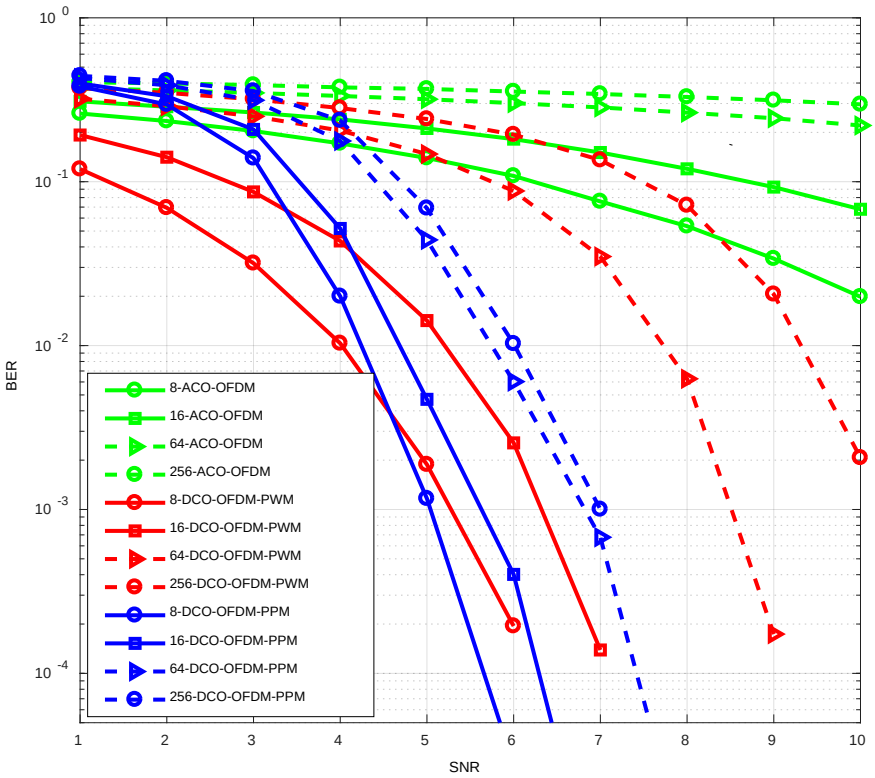

Figure 7: BER against the SNR for original ACO-OFDM, DCO-OFDM-PWM and DCO-OFDM-PPM for an ideal LOS channel (N_{SC}=256, L=100).

The BER performance against SNR for DCO-OFDM-PTM and ACO-OFDM for 8-, 16- 64-, and 256-QAM and a LOS channel are illustrated in Figure 7. The channel is considered to be ideal with AWGN with no reflections. As is seen for all orders of modulation, DCO-OFDM-PTM schemes require lower SNR values than ACO-OFDM, with DCO-OFDM-PPM offering the best performance. For example, for 8-, 16-, 64-, and 256-QAM and at the BER of 10^{-3}, the SNR gains are ~0.3, ~0.7, ~1.65, and ~3.5 dB for DCO-OFDM-PPM compared with DCO-OFDM-PWM, respectively. Note that, for ACO-OFDM, the power penalties are very high. The BER performance against SNR for 16- and 64- DCO-OFDM-PTM and ACO-OFDM-PTM schemes for the ideal LOS channel is depicted in Figure 8. Based on this figure, the use of DCO-OFDM samples offers improved BER performance compared with ACO-OFDM-PTM. For instance, for 16-QAM and at the BER of 10^{-3}, the SNR gains are ~1.35 and ~1 dB for DCO-OFDM-PPM and DCO-OFDM-PWM compared to ACO-OFDM-PPM and ACO-OFDM-PWM, respectively.

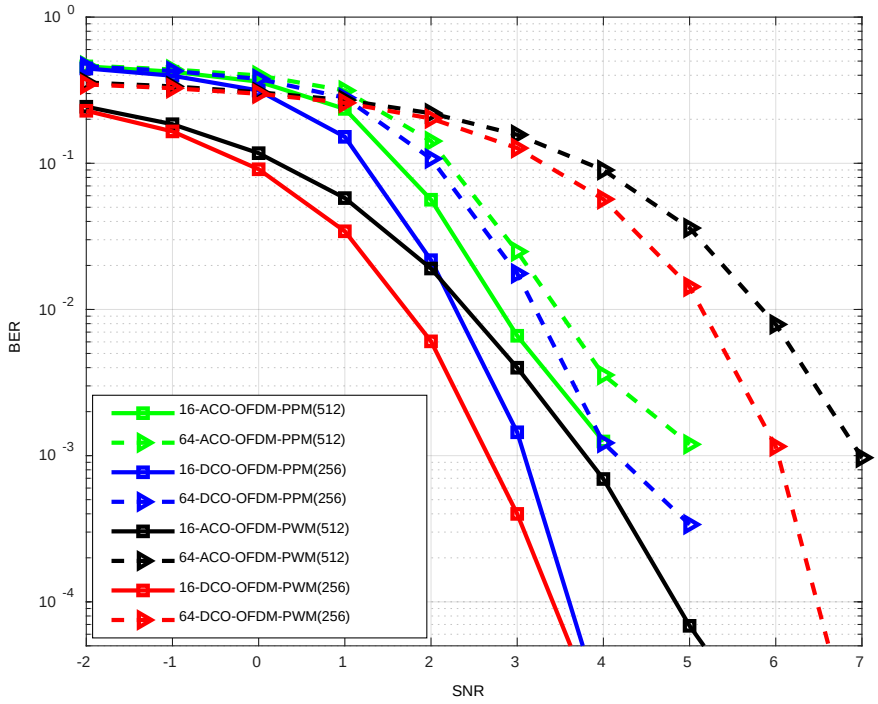

Figure 8: BER performance against the SNR for DCO-OFDM-PWM/PPM and ACO-OFDM-PWM/PPM for an ideal LOS channel (N_{SC} for ACO-OFDM-PTM and DCO-OFDM-PTM are 512 and 256 respectively, L for ACO-OFDM-PTM and DCO-OFDM-PTM are 500 and 200, respectively)

The BER performance against the SNR for DCO-OFDM-PWM and DCO-OFDM-PPM for the non-ideal channel for configurations (a) and (b) are presented in Figure 9. In the simulation of the non-ideal channel, all reflections from walls as well as AWGN are considered. Key channel parameters are given in Table 2. Unlike configuration (b), there is a strong LOS component in Configuration (a). In this case, for all orders of modulation, the DCO-OFDM-PPM scheme requires lower SNR values compared to DCO-OFDM-PWM. For example, for 4-, 8-, and 16-QAM and at the BER of 10^{-3}, the SNR gains are ~1.5, ~4.5, and ~5.8 dB, respectively, for DCO-OFDM-PPM compared with DCO-OFDM-PWM. Also, the BER performance of DCO-OFDM-PWM for 64- and 256-QAM severely deteriorates compared with DCO-OFDM-PPM. In configuration (b), the BER performance of DCO-OFDM-PPM for 8-, 16-, 64-, and 256-QAM is improved compared with DCO-OFDM-PWM. For instance, for 8- and 16-QAM and at the BER of 10^{-3}, the SNR gains of DCO-OFDM-PPM are ~ 0.8 and ~ 1.9 dB, respectively, compared with DCO-OFDM-PWM.

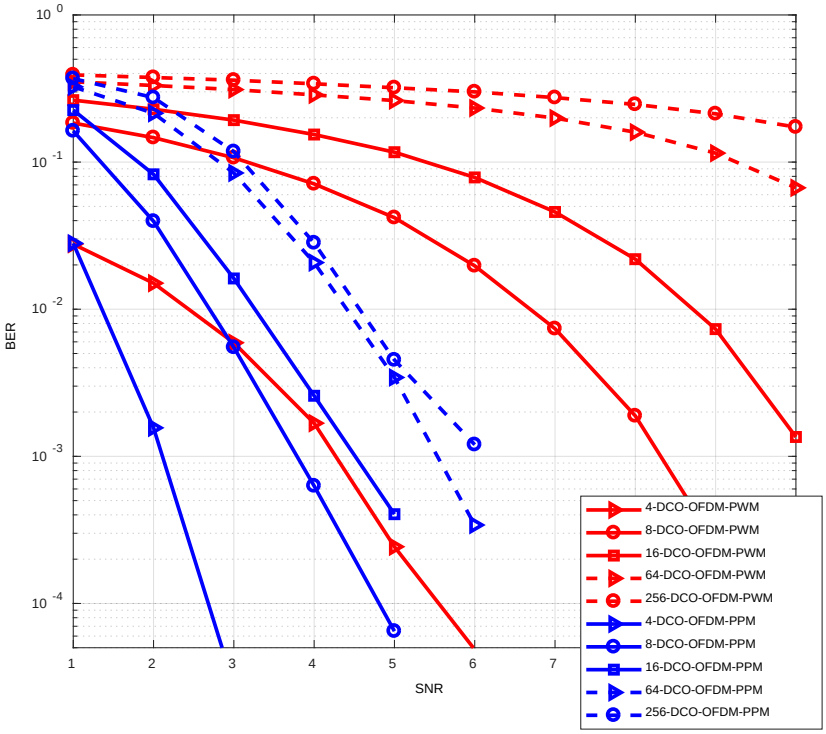

(a)

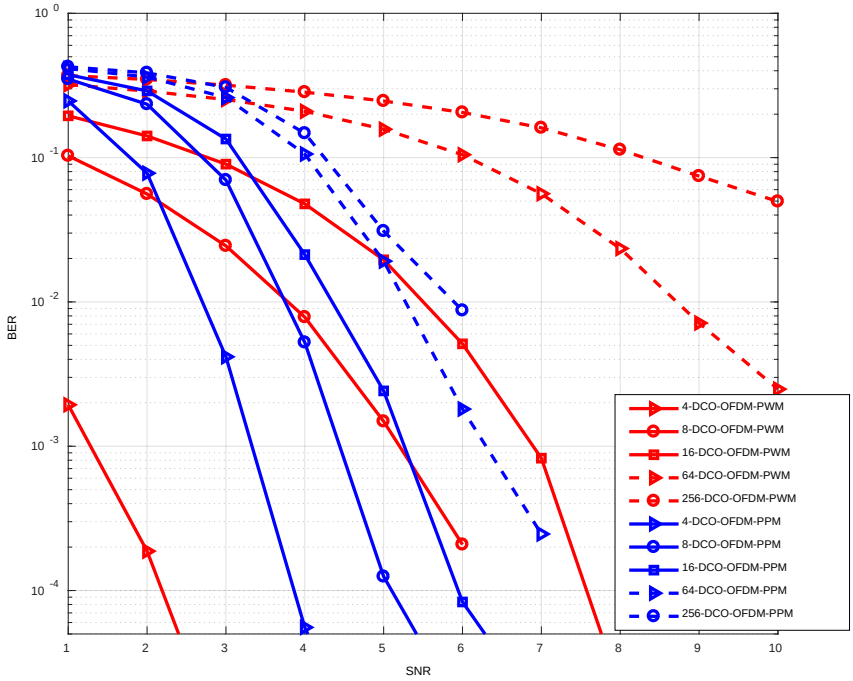

(b)

Figure 9: BER against the SNR for DCO-OFDM-PWM and DCO-OFDM-PPM with N_{SC}=256, and L=100 for the diffuse channel: (a) for the room configuration Fig. 3(a), and (b) for the room configuration Fig. 3(b

The number of sampling points of OFDM in OFDM-PTM is very important. By reducing the sampling points (number of OFDM sampling points < number of IFFT points), the error is greatly increased. The effect of a drop in the number of OFDM sampling points on the BER performance of DCO-OFDM-PWM for 8-, 16-, and 64-QAM in the ideal LOS channel is shown in Figure 10.

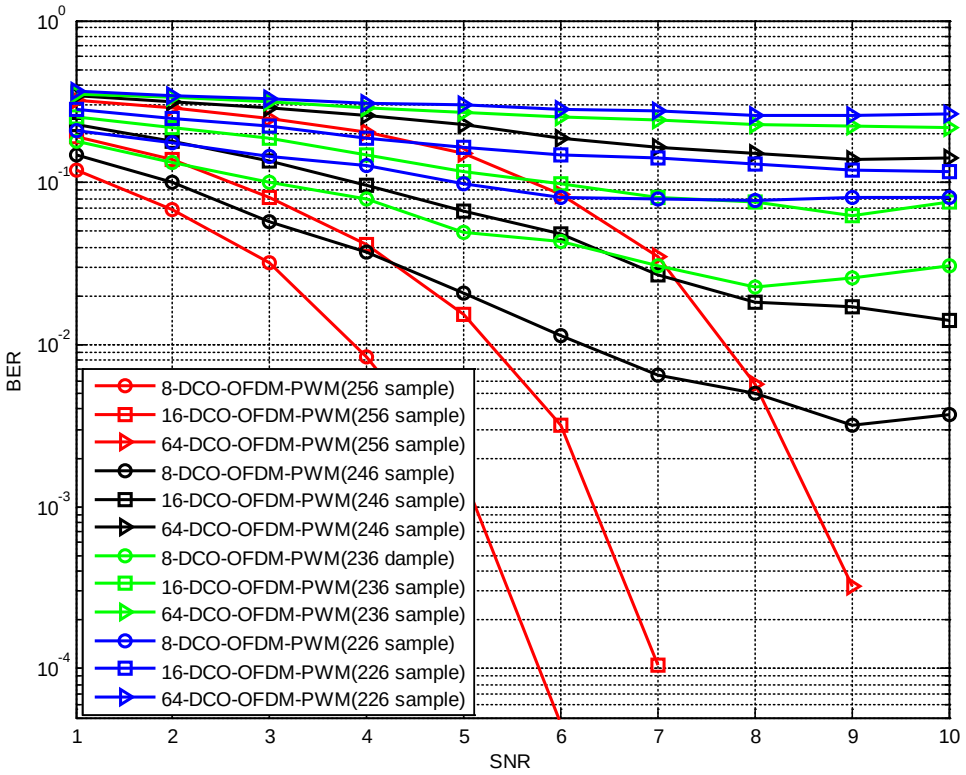

Figure 10: The BER performance against the SNR for DCO-OFDM-PWM with different number of OFDM sampling points for an ideal LOS channel (N_{SC}=256, L=100).

Table 2: Channel simulation parameters

Parameter	Value
Room size	5×5×3
Reflection coefficient	0.8
Semi-angle at half power	70
Active area	1
Half angle FOV	60

4. Conclusion

In this paper, we described a hybrid DCO-OFDM-PTM scheme (i.e. DCO-OFDM-PWM and DCO-OFDM-PPM) for both the ideal line of sight and diffuse channel conditions, which offered a lower PAPR and improved BER compared with the original ACO-OFDM and ACO-OFDM-PTM. We demonstrated that the BER performance of DCO-OFDM-PPM is better than that of DCO-OFDM-PWM, especially for higher-order modulations. At the BER of 10^{-3}, for 8- and 16-QAM-based DCO-OFDM-PPM, the SNR gains were ~0.8 and ~1.9 dB, respectively, compared with DCO-OFDM-PWM.

References

[1] J. H Reed, J. T. Bernhard, and J. Park. "Spectrum access technologies: The past, the present, and the future", *Proceedings of the IEEE*, vol.100, pp. 1676-1684, 2012.

[2] Z. Ghassemlooy, S. Arnon, M. Uysal, X. zhengyuan, and C. Julian, "Emerging Optical Wireless Communication Advances and Challenges", *Sel. Areas Commun. IEEE J.*, vol. 33, pp. 1738-1749, 2015.

[3] P. Anthony Haigh, Z.Ghassemlooy, S. Rajbhandari, and L. Papakonstantinou, "Visible Light Communications Using Organic Light Emitting Diodes", *IEEE Communications J.*, vol. 51, no. 8, pp. 148-154, 2013.

[4] Y. Tanaka, T. Komine, S. Haruyama, and M. Nakagawa, "Indoor Visible Light Data Transmission System Utilizing White LED Lights", *IEICE Transactions on Communications*, vol. E86-B, no. 8, pp. 2440–2454, 2003.

[5] B. Inan, S. C. J. Lee, S. Randel, I. Neokosmidis, A. M. J. Koonen and J. W. Walewski, "The impact of LED transfer function nonlinearity on high-speed optical wireless communications based on discrete-multitone modulation," *2009 Conference on Optical Fiber Communication - incudes post deadline papers*, San Diego, CA, pp. 1-3, 2009.

[6] J. Armstrong, "OFDM for Optical Communications,"*Journal of Lightwave Technology*, vol. 27, no. 3, pp. 189–204, 2009.

[7] S. D. Dissanayake, J. Armstrong, "Comparison of ACO-OFDM, DCO-OFDM and ADO-OFDM in IM/DD systems", *J. Lightwave Technol*, vol. 31, no. 7, pp. 1063–1072, 2013.

[8] K. Werfli, P.A. Haigh, and Z. Ghassemlooy, "Multi-band carrier-less amplitude and phase modulation with decision feedback equalization for bandlimited VLC systems", *Optical Wireless Communications (IWOW)*, 2015 4th International Workshop on IEEE, pp. 6–10, 2015.
[9] J. Vucic, C. Kottke, S. Nerreter, K. D. Langer, and J. W. Walewski, "513 Mbit/s Visible Light Communications Link Based on DMT-Modulation of a White LED,"*Journal of Lightwave Technology*, vol. 28, no. 24, pp. 3512–3518, 2010.
[10] C. H. Yeh, H. Y. Chen, et al, "Utilization of multi-band OFDM modulation to increase traffic rate of phosphor-LED wireless VLC," *Opt. Express 23*, no. 2, pp. 1133-1138, 2015.
[11] K. Ying, H. Qian, RJ. Baxley and S.Yao, "Joint optimization of precoder and equalizer in MIMO VLC systems." *IEEE Journal on Selected Areas in Communications* ,vol. 33, no. 9, pp. 1949-1958, 2015.
[12] R. Jiang, Z. Wang, Q.Wang and L. Dai, "Multi-User Sum-Rate Optimization for Visible Communications with Lighting Constraints." *Journal of Lightwave Technology* vol. 34, no. 16, pp. 3943-3952, 2016.
[13] P. P. Han, A. Sewaiwar, S. V. Tiwari and Y. H. Chung, "Color clustered multiple-input multiple-output visible light communication*", Journal of the Optical Society of Korea*, vol. 19, no.1, pp. 74-79, 2015.
[14] P. A. Haigh, F. Bausi, T. Kanesan, S. T. Le, S. Rajbhandari, Z. Ghassemlooy, I. Papakonstantinou, W. Popoola, A. Burton, H. L. Minh, A. D. Ellis, and F. Cacialli, "A 20-Mb/s VLC link with a polymer LED and a multilayer perceptron equalizer," *IEEE Photonics Technology Letters*, vol. 26, no. 19, pp. 1975 – 1978, 2014.
[15] C. W. Hsu, Y. Ksu, et al "Mitigation of LED Nonlinearity Using Adaptive Equalization for Visible Light Communications," *in ACP, OSA Technical Digest*, pp. Su2A-52, 2017.
[16] J. Y. Sung, C. W. Chow, and C. H. Yeh, "Is blue optical filter necessary in high speed phosphor-based white light LED visible light communications?," *Opt. Express, vol.* 22, no. 17, pp. 20646-20651, 2014.
[17] P. A. Haigh, F. Bausi, H. Le Minh, I. Papakonstantinou, W. O. Popoola, A. Burton and F. Cacialli, "Wavelength-Multiplexed Polymer LEDs: Towards 55 Mb/s Organic Visible Light Communications", Selected Areas in Communications, *IEEE Journal on*, vol. 33, no. 9, 2015.
[18] R. X. J. Ferreira, E. Xie, J. J. D. Mckendry, S. Ranjbhandari, H.chun, D. C. O'Brien and M. D. dawson, "High bandwidth GaN-based micro-LEDs for multi-Gbps visible light communications", *IEEE Photonics Technol. Lett.,* vol. 28. No. 19, pp. 2023-2026, 2016.
[19] K. Asatani and T. Kimura, "Linearization of LED nonlinearity by Predistortions," *IEEE Journal of Solid-State Circuits,* vol. 13, no. 1, pp. 133–138, February 1978.
[20] G. Stepniak, J. Siuzdak, and P. Zwierko, "Compensation of a VLC Phosphorescent White LED Nonlinearity by Means of Volterra DFE," *IEEE Photonics Technology Letters*, vol. 25, no. 16, pp. 1597–1600, August 2013.
[21] H. Qian, S. J. Yao, S. Z. Cai, and T. Zhou, :Adaptive Post-Distortion for Nonlinear LEDs in Visible Light Communications*", IEEE Photonics Journal*, vol. 6, no. 4, 2014.
[22] S. Dimitrov and H. Haas, "On the Clipping Noise in an ACO-OFDM Optical Wireless Communication System", *Proceedings of the IEEE Global Communications Conference (IEEE GLOBECOM 2010)*, Miami, FL, 2010.
[23] T. Tao Jiang and Y. Yiyan Wu, "An Overview: Peak-to-Average Power Ratio Reduction Techniques for OFDM Signals," *IEEE Trans. Broadcast.*, vol. 54, no. 2, pp. 257–268, Jun. 2008.
[24] T. Tao Jiang, Y. Yiyan Wu, "An Overview: peak-to-average power ratio reduction techniques for OFDM Signals", *IEEE Trans. Broadcast*. Vol. 54, 257–268 2013.
[25] F. Ogunkoya, O. Popoola, A. Shahrabi, and S. Sinanovic. "Performance evaluation of pilot-assisted PAPR reduction technique in optical OFDM systems." *IEEE Photonics Technology,* vol. 27, no. 10, pp. 1088-1091, 2015.
[26] D. Abed, and A. Medjouri. "Discrete sliding norm transform-based 50% PAPR reduction in asymmetrically clipped optical OFDM systems for optical wireless communications." *Electronics Letters,* vol. 51, no. 25, pp. 2128-2130, 2015.
[27] M. Z. Farooqui, P. Saengudomlert, and S. Kaiser. "Average transmit power reduction in OFDM-based indoor wireless optical communications using SLM." *Electrical and Computer Engineering (ICECE), 2010 International Conference on*. IEEE, 2010.
[28] Amol J. Bhaktea, and Kiran D. Bondreb. "DFT-Spread combined with PTS and SLM method to reduce the PAPR in VLC-OFDM system." *International journal of Advanced Research in Electronics & Communication Engineering*, vol. 5, no.4, pp. 1027-1030, 2016.
[29] B. Yu, H. Zhang, L. Wei and J. Song, "Subcarrier grouping OFDM for visible-light communication systems." *IEEE Photonics Journal*, vol. 7, no. 5, pp. 1-12, 2015.
[30] P. Chvojka, S. Zvanovec, P. A. Haigh, Z. Ghassemlooy, "Channel characteristics of visible light communications within dynamic indoor environment." *Journal of Lightwave Technology,* vol. 33, no.9, pp. 1719-1725, 2015.
[31] T. Zhang, Z. Ghassemlooy, S.Rajbhandari, W. O. Popoola, S. Guo "OFDM-PWM scheme for visible light communications." *Optics Communications*, vol. 385, pp. 213-218, 2017.
[32] B. Wilson, and Z. Ghassemlooy. "Pulse time modulation techniques for optical communications: a review." *IEE Proceedings J (Optoelectronics)*, vol. 140, no. 6, pp. 346-358, 1993.
[33] Z. Ghassemlooy, W.O. Popoola, S. Rajbhandari, "Optical Wireless Communications System and Channel Modelling with Matlab", CRC Publisher, New York, USA, 2012.
[34] S. Rajagopal, R. D. Roberts and S. K. Lim, "IEEE 802.15.7 visible light communication: modulation schemes and dimming support," in IEEE Communications Magazine, vol. 50, no. 3, pp. 72-82, March 2012.
[35] W. Shieh and I. Djordjevic, Orthogonal Frequency Division Multiplexing for Optical Communications, Academic Press, 18 Sep. 2009
[36] R. J. Baxley and G. T. Zhou, "Peak-to-Average Power Ratio Reduction," in Digital Signal Processing Handbook, 2nd ed., V. Madisetti, Ed. CRC Press, 2009.

[37] Z. Ghassemlooy, F. Ebrahimi, S. Rajbhandari, S. Olyaee, X. Tang, and S. Zvanovec, "Hybrid OFDM-PTM based Visible Light Communications-Invited Paper", The 13th International Wireless Communications and Mobile Computing Conference (IWCMC 2017), Valencia, Spain; 26-30 June, 2017.